THE JOURNAL OF BIOLOGICAL CHEMISTRY
Vol. 274, No. 53, Issue of December 31, pp. 37974–37981, 1999
Printed in U.S.A.

Mutation of Arg-54 Strongly Influences Heme Composition and Rate and Directionality of Electron Transfer in *Paracoccus denitrificans* Cytochrome *c* Oxidase*

(Received for publication, July 12, 1999, and in revised form, September 2, 1999)

Aimo Kannt‡, Ute Pfitzner§, Maarten Ruitenberg¶, Petra Hellwig‖, Bernd Ludwig§, Werner Mäntele‖, Klaus Fendler¶, and Hartmut Michel‡**

From the ‡Max-Planck-Institut für Biophysik, Abteilung Molekulare Membranbiologie, Heinrich-Hoffmann-Straße 7, D-60528, the §Molekulare Genetik, Institut für Biochemie an der Johann-Wolfgang-Goethe-Universität, Marie-Curie-Straße 9, D-60439, ‖Institut für Biophysik an der Johann-Wolfgang-Goethe-Universität, Theodor-Stern-Kai 7, Haus 74, D-60590, and ¶Max-Planck-Institut für Biophysik, Abteilung Biophysikalische Chemie, Kennedyallee 70, D-60596 Frankfurt/Main, Germany

The effect of a single site mutation of Arg-54 to methionine in *Paracoccus denitrificans* cytochrome *c* oxidase was studied using a combination of optical spectroscopy, electrochemical and rapid kinetics techniques, and time-resolved measurements of electrical membrane potential. The mutation resulted in a blue-shift of the heme *a* α-band by 15 nm and partial occupation of the low-spin heme site by heme O. Additionally, there was a marked decrease in the midpoint potential of the low-spin heme, resulting in slow reduction of this heme species. A stopped-flow investigation of the reaction with ferrocytochrome *c* yielded a kinetic difference spectrum resembling that of heme a_3. This observation, and the absence of transient absorbance changes at the corresponding wavelength of the low-spin heme, suggests that, in the mutant enzyme, electron transfer from Cu_A to the binuclear center may not occur via heme *a* but that instead direct electron transfer to the high-spin heme is the dominating process. This was supported by charge translocation measurements where $\Delta\psi$ generation was completely inhibited in the presence of KCN. Our results thus provide an example for how the interplay between protein and cofactors can modulate the functional properties of the enzyme complex.

Cytochrome *c* oxidase (*cf.* Ref. 1 for a recent review), the terminal enzyme of the respiratory chain of mitochondria and many aerobic bacteria, catalyzes electron transfer from cytochrome *c* to molecular oxygen thereby reducing the latter to water. The redox reaction is coupled to proton translocation across the inner mitochondrial or bacterial membrane, resulting in an electrochemical proton gradient, $\Delta\mu_{H^+}$, across the membrane as shown in Reaction 1.

$$4\ \text{cyt}\ c^{2+} + 8\ H^+_i + O_2 \rightarrow 4\ \text{cyt}\ c^{3+} + 4\ H^+_o + 2\ H_2O$$

REACTION 1

H^+_i denotes protons taken up from the inner phase (the mitochondrial matrix or bacterial cytoplasm), whereas H^+_o refers to protons released into the outer phase (the intermembrane space or periplasm).

Four metal centers participate in electron transfer from cytochrome *c* to oxygen. The first electron acceptor is Cu_A, a homodinuclear copper center bound to subunit II. From there, electrons are transferred to the low-spin heme *a* and then to the heme a_3-Cu_B binuclear center, where oxygen reduction takes place.

Cytochrome *c*-Cu_A electron transfer occurs at a rate of 70,000 s^{-1} (2, 3). The rate-limiting step for reduction of Cu_A, however, is the binding of cytochrome *c* that is strongly dependent on ionic strength (4, 5). From Cu_A, electrons are rapidly transferred to heme *a*, at a rate of $\approx 10^4\ s^{-1}$ (6, 7). Considering the relatively long metal-to-metal distance of 19.5 Å (8) and the small driving force of ≈50 mV (9), this electron transfer is remarkably fast. This has been attributed to a combination of small reorganization energy due to the binuclear structure of Cu_A (10) and the presence of an efficient electron transfer pathway between the two metal centers (11, 12). In contrast, electron transfer from Cu_A directly to heme a_3 is negligibly slow (1–100 s^{-1}, 13), due to the longer metal-to-metal distance of 22.1 Å, a higher reorganization energy resulting from the more polar environment around heme a_3 (13), and a less favorable tunneling pathway (12). Further electron transfer from heme *a* to heme a_3 is intrinsically fast as the two metal atoms are only 13.5 Å apart and the edge-to-edge distance of the two hemes is only 4.5 Å. However, the rate of this process is controlled by simultaneous proton uptake stabilizing the reduced heme a_3 (14) and is also critically dependent on the redox state of the enzyme. Reported rates range from $<10\ s^{-1}$ for anaerobic reduction of the oxidized enzyme (15) to $2 \times 10^4\ s^{-1}$ in the reaction of the fully reduced enzyme with dioxygen (7). A rate of $3 \times 10^5\ s^{-1}$ was reported for the $a_3 \rightarrow a$ reverse electron transfer after CO dissociation from the mixed valence enzyme (16, 17). So far, the importance of the "diversion" of electron transfer to the binuclear center via the low-spin heme is still unclear. It has recently been suggested that heme *a* plays a critical role in the coupling of electron transfer to proton translocation (18–21).

In this study, we have investigated the effect of the mutation of a single amino acid, Arg-54, to methionine. Arg-54 is conserved among cytochrome *c* oxidases that contain an A-type heme in the low-spin site. The crystal structures of both the *Paracoccus denitrificans* (8, 22) and bovine heart (23) enzymes show that Arg-54 is located close to the low-spin heme forming a strong hydrogen bond to the formyl group of the heme (*cf.* Fig. 1). From electrostatic calculations (24) it could be deduced that the arginine, although being buried within the protein, is pro-

* This work was supported by the Deutsche Forschungsgemeinschaft (SFB 472, TP 9/8/1). The costs of publication of this article were defrayed in part by the payment of page charges. This article must therefore be hereby marked "*advertisement*" in accordance with 18 U.S.C. Section 1734 solely to indicate this fact.

** To whom correspondence should be addressed. Tel.: 49 69 96769-400; Fax: 49 69 96769-423; E-mail: Michel@mpibp-frankfurt.mpg.de.

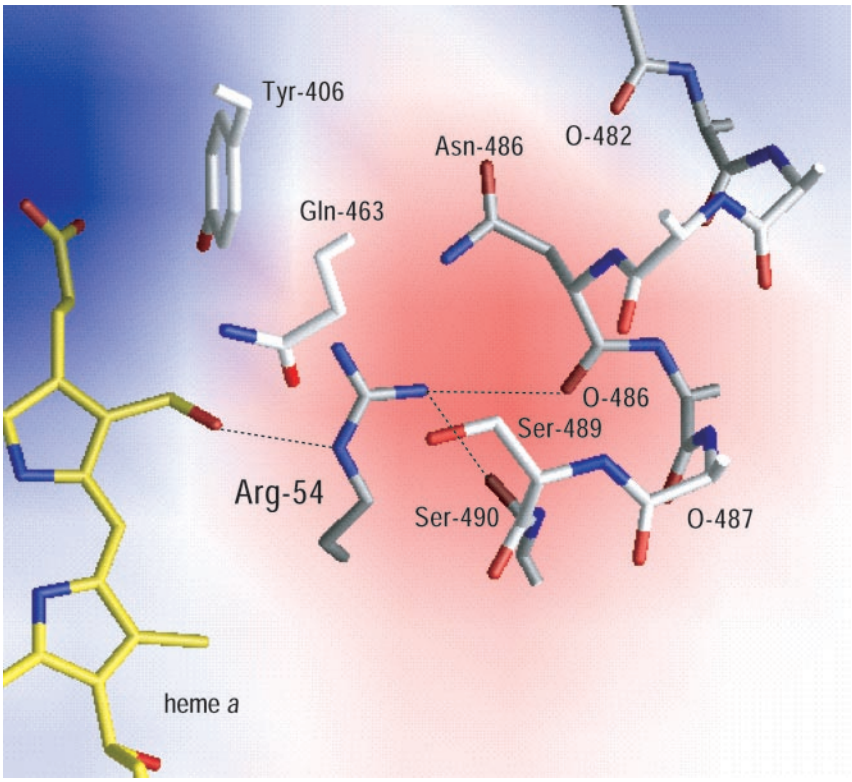

FIG. 1. **Environment of Arg-54 in *P. denitrificans* cytochrome *c* oxidase.** The guanidino group of the arginine is hydrogen-bonded to the formyl group of heme *a*, the backbone carbonyl oxygen of residue 486, and the hydroxyl group of Ser-490 (*dotted lines*). The polar side chains of Gln-463, Ser-489, and Ser-490 and the backbone carbonyl dipoles of residues 482, 483, 486, and 487 that are oriented with their carbonyl oxygen atoms pointing toward Arg-54 create a region of negative potential (*red*) stabilizing the positive charge on the arginine. The figure was adapted from Ref. 52, prepared with GRASP (53).

tonated, and that the positive charge has a strong influence on the redox potential of the low-spin heme. The interaction energy was calculated as 23.7 kJ/mol, corresponding to 245 meV. It was therefore to be expected that replacement of the arginine by a neutral residue would have a strong effect on the redox properties of the heme. In the following, it will be shown that mutation of Arg-54 to methionine yields an enzyme with altered spectral properties, different heme composition, a drastically lowered midpoint potential of heme *a*, and, correspondingly, a dominance of direct Cu_A-heme a_3 electron transfer over the "normal" pathway of electron transfer.

EXPERIMENTAL PROCEDURES

Enzyme Preparation—Site-directed mutagenesis on *P. denitrificans* cytochrome aa_3 was performed as described (25). Bacteria were grown in succinate medium (26) at 32 °C, and cells were harvested at the late exponential phase. Bacterial membranes were isolated as described (27) and solubilized with *n*-dodecyl-β-D-maltopyranoside (28). Cytochrome *c* oxidase was then purified by streptavidin affinity chromatography as described by Kleymann *et al.* (28), using an engineered streptavidin (29). The steady-state activity of the mutant enzyme was determined spectrophotometrically by following the oxidation of horse heart cytochrome *c* (Biomol, Hamburg, Germany) as the change in absorbance at 550 nm. The measurement was performed in 10 mM potassium phosphate, pH 7.0, 40 mM KCl, 0.05% *n*-dodecyl-β-D-maltopyranoside, and the cytochrome *c* concentration was 50 μM.

Spectra of CO Derivatives—For the generation of the CO-ligated mixed valence enzyme, the oxidized cytochrome *c* oxidase was diluted in 50 mM Hepes-KOH, pH 7.4, 0.05% *n*-dodecyl-β-D-maltopyranoside, to a concentration of ≈5 μM in an optical cuvette. After addition of 25 μg/ml catalase, 150 mM β-D-glucose, and 40 μg/ml glucose oxidase, the solution was degassed using a vacuum pump and flushed with argon. After recording a spectrum of the oxidized enzyme, the argon was replaced by CO. Formation of the CO-ligated mixed valence enzyme was monitored spectrophotometrically and was complete after ≈3 h incubation at room temperature. After recording the "oxidized + CO" spectrum, the enzyme was reduced by adding a few grains of sodium dithionite and again equilibrated with CO. In the case of the wild-type enzyme, formation of the "reduced + CO" species occurred nearly instantaneously, whereas it took up to several hours for the R54M mutant enzyme (see "Results"). For the determination of the reduced-minus-(reduced + CO) spectrum, the procedure was as described above, except that the enzyme was reduced and the spectrum of the reduced enzyme was recorded prior to incubation with CO.

Pyridine Hemochrome Spectra—Alkaline pyridine hemochrome spectra were measured as described (30). The protein was dissolved in a 3:1 mixture of 0.2 M NaOH and pyridine containing 0.5 mM $K_3[Fe(CN)_6]$. After recording the ferrihemochrome spectrum, the sample was reduced by addition of a few grains of solid sodium dithionite, and several successive spectra of the developing ferrohemochrome were recorded until no further changes were detectable. The concentrations of different heme species were determined using the following extinction coefficients for the reduced-minus-oxidized difference spectra (31): $\epsilon_{587-620}$ = 25 mM^{-1} cm^{-1} for heme A and $\epsilon_{552-536}$ = 24 mM^{-1} cm^{-1} for heme O. The latter value was based on the assumption that the peak-to-trough absorbance difference is similar for hemes B and O (32).

HPLC[1] Heme Analysis—Hemes were extracted from the isolated enzyme complexes essentially as described (33, 34). After precipitation with 10 volumes of 90% acetone, 10% water, 10 mM NH_3, the hemes were extracted from the pellet first into acetone/HCl/water (90:2:8, v/v) and then into diethyl ether. The ether was evaporated, and the hemes were redissolved in a small volume of ethanol/acetic acid/water (90:17:13, v/v). HPLC analysis was done using the same solvent as the mobile phase on a C_{18} reverse phase column (Latek Spherisorb ODS-1, 5 μ, 250 × 4 mm) at a flow rate of 0.5 ml/min. Eluted hemes were detected optically by following their absorbance at 402 nm.

Electrochemically Induced Difference Spectra and Redox Potential Determination—Electrochemically induced oxidized-minus-reduced difference spectra in the visible range were obtained and electrochemical redox titrations carried out as described by Hellwig *et al.* (35).

BLM Experiments—Optically black lipid membranes were formed in a thermostated (25 °C) Teflon cell filled with an electrolyte solution (1.3 ml in each compartment) as described by Bamberg *et al.* (36), and voltage measurements were performed as outlined by Hartung *et al.* (37). The membrane-forming solution contained 1.5% (w/v) diphytanoyl lecithin (Avanti Biochemicals, Birmingham, AL) and 0.025% (w/v) octadecylamine (Riedel-de-Haen, Hannover, Germany) in *n*-decane. Cytochrome *c* oxidase containing vesicles were prepared using *Escherichia coli* lipids (acetone/ether preparation, Avanti) at a lipid/protein ratio of 20 (w/w). The reconstitution procedure was as described by Gropp *et al.* (38), with 2% (w/v) sodium cholate as detergent in 50 mM Hepes-KOH, pH 7.4.

[1] The abbreviations used are: BLM, black lipid membrane; Rubpy, $Ru^{II}(2, 2'\text{-bipyridyl})_3Cl_2$; HPLC, high pressure liquid chromatography.

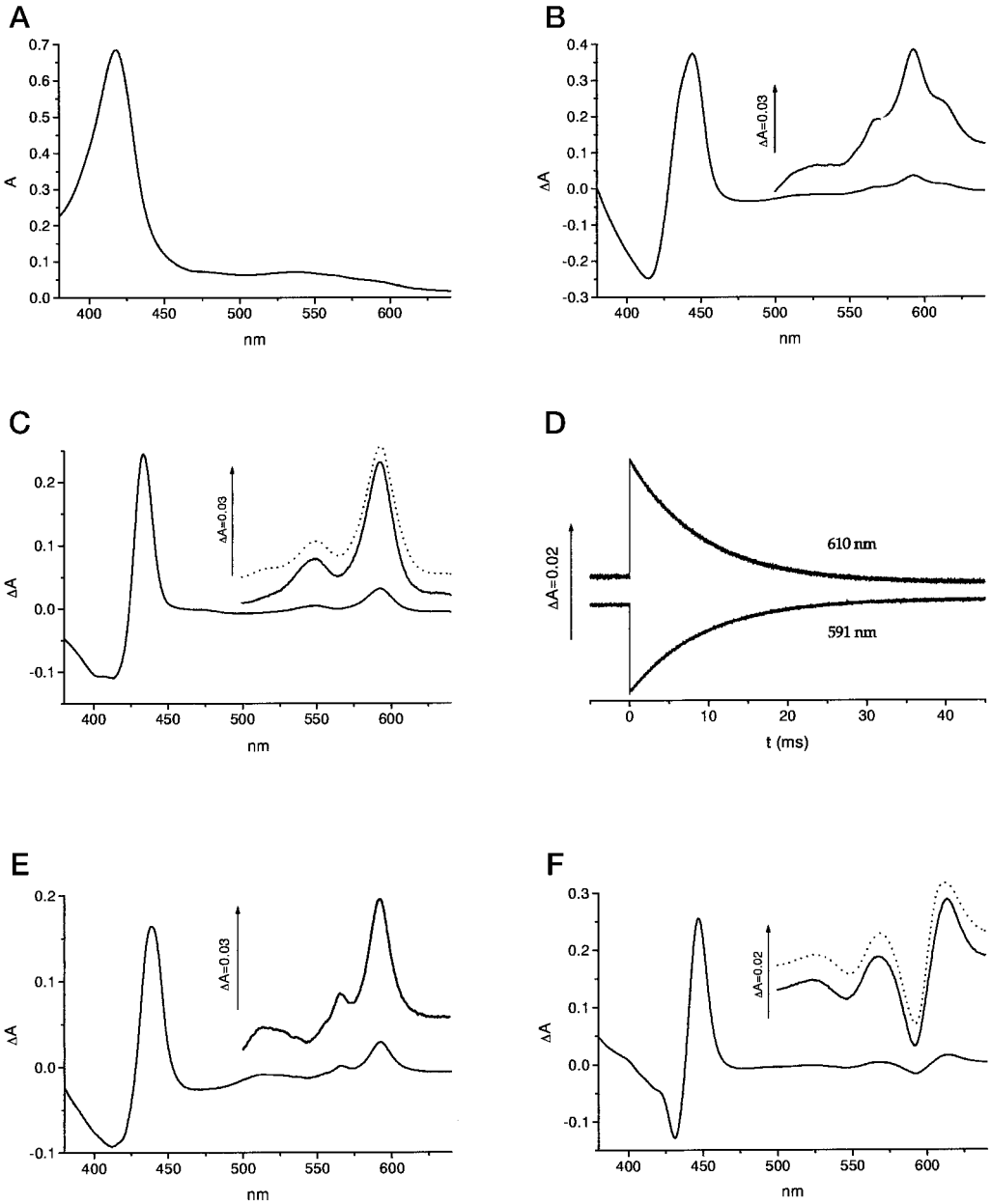

FIG. 2. **Absorbance spectra of R54M mutant cytochrome *c* oxidase.** *A,* oxidized enzyme. *B,* reduced-minus-oxidized difference spectrum. *C,* (oxidized + CO)-minus-(oxidized) difference spectrum. *D,* CO recombination kinetics in the CO-ligated mixed valence enzyme. CO was photolysed by a 308 nm laser flash, and rebinding was monitored at the indicated wavelengths. *E,* (reduced + CO)-minus-(oxidized + CO) difference spectrum. *F,* reduced-minus-(reduced + CO) difference spectrum. *Dotted lines* in *C* and *F* show the corresponding spectra of the wild-type enzyme. In all cases, the buffer was 50 mM Hepes-KOH, 0.05% *n*-doclecyl-β-D-maltopyramoside, pH 7.4, and the enzyme concentration was 4.3 μM except for *D* where it was 10 μM.

Both compartments of the Teflon cell, connected to an external measuring circuit via platinum electrodes, were filled with 50 mM Hepes-KOH, pH 7.4, and cytochrome *c* oxidase containing vesicles were added to a concentration of 120 nM to one of the compartments. The vesicles were allowed to adsorb to the BLM by incubation for >60 min under stirring, yielding a capacitive coupling between proteoliposomes and the measuring system, as illustrated in Ref. 37. Eighty μM Rubpy and 300 μM EDTA were added to the same compartment. The ruthenium derivative was excited by a short laser pulse delivered from an excimer laser pumped dye laser (451 nm, 160 mJ/cm^2), resulting in rapid electron injection into the enzyme (39). EDTA acts as a sacrificial electron donor that re-reduces the generated Ru(III)bpy thus making electron injection into cytochrome *c* oxidase irreversible. The resulting voltage signal was amplified (1000 ×), filtered (DC to 1 MHz), and recorded with a digital oscilloscope (Nicolet Integra 10). The input of the voltage amplifier was shunted by a 1 GΩ resistor.

Pre-steady-state Kinetics—Five μM reduced horse heart cytochrome *c* (Biomol) and 5 μM cytochrome *c* oxidase were mixed 1:1 in a Hi-Tech Scientific stopped-flow spectrophotometer at 25 °C in 50 mM Hepes-KOH, pH 7.3, 120 mM KCl, 0.05% *n*-dodecyl-β-D-maltopyranoside. The reaction was followed at 550 nm (cytochrome *c* oxidation) and between 580 and 620 nm (cytochrome aa_3 reduction). For the determination of kinetic difference spectra in the region between 580 and 620 nm, the maximal changes in absorbance were corrected for the contribution from cytochrome *c* and plotted against the corresponding wavelengths.

RESULTS

Enzymatic Activity and Spectral Characteristics—Substitution of Arg-54 by methionine yielded an enzyme with a turnover number of 8 s^{-1}. This corresponds to 2% of the activity determined for the wild-type *P. denitrificans* cytochrome *c* oxidase. The optical absorption spectrum of the R54M mutant enzyme differs significantly from that of the wild-type enzyme (*cf.* Fig. 2 and Table I): In the α-band region of the reduced-

TABLE I

α-Band signals observed in the optical difference spectra of R54M and its CO derivatives

See also Figure 3.12. Numbers in parentheses refer to the wavelengths of the corresponding bands observed for the wild-type enzyme.

Difference spectrum	Signals	Assignment
Reduced-minus-oxidized	612 nm (607)[a]	Reduced high-spin heme
	592 nm	Reduced low-spin heme
(Oxidized + CO)-minus-oxidized	592 nm (592.5)	Reduced, CO-ligated high-spin heme
(Reduced + CO)-minus-(oxidized + CO)	592 nm (607)	Reduced low-spin heme
Reduced-minus-(reduced + CO)	Peak at 612 nm (612)	Reduced high-spin heme
	Trough at 592 nm (592.5)	CO dissociation from the reduced high-spin heme

[a] Due to the spectral overlap, the respective contributions of hemes *a* and a_3 are not resolved in the reduced-minus-oxidized difference spectrum of the wild-type enzyme.

minus-oxidized spectrum, there is a maximum at 592 nm with two shoulders at 566 and 612 nm (Fig. 2*B*). Assignment of these signals to different heme species was done using two independent approaches: by recording spectra of CO-derivatives and by separating the heme contributions electrochemically. As shown in Fig. 2*E*, the 592-nm species is also observed in the (reduced + CO)-minus(oxidized + CO) spectrum indicating that it is associated with the low-spin heme. The 612-nm signal, in turn, is observed in the reduced-minus-(reduced + CO) spectrum (Fig. 2*F*) in which there is also a trough at 592 nm, suggesting that the 612-nm band is due to reduced heme a_3 and shifts to 592 nm upon binding of CO. This is confirmed by the (oxidized + CO)-minus-oxidized spectrum (Fig. 2*C*) in which there is a peak at 592 nm due to the reduced, CO-ligated heme a_3. This assignment was verified by studying the CO recombination kinetics. When CO was dissociated from the mixed valence enzyme by a strong laser pulse (Fig. 2*D*), a rapid decrease in absorbance at 591 nm was observed. CO recombination, *i.e.* restoration of the signal, occurred at a rate of 110 s^{-1}. At 610 nm, *i.e.* close to the absorbance maximum of the unligated heme a_3, the opposite was observed as follows: a rapid increase in absorbance concurrent with CO dissociation, followed by a decrease to the original absorbance value at a rate of 110 s^{-1}. It can thus be concluded that the 592-nm signal in the reduced-minus-oxidized spectrum of R54M is associated with the low-spin heme, whereas the 612-nm band is due to the high-spin heme and shifts to 592 nm upon binding of CO. Thus, whereas the heme a_3 spectrum is nearly indistinguishable from the corresponding absorption spectrum of the wild-type *P. denitrificans* cytochrome *c* oxidase, the heme *a* maximum is blue-shifted by about 15 nm (see "Discussion"). Separation of the heme contributions in the electrochemically induced oxidized-minus-reduced difference spectra yielded the same results, as shown below in Fig. 4.

As mentioned above, there is a shoulder at 566 nm in the reduced-minus-oxidized difference spectrum of R54M. In part, this signal is also observed, although less pronounced, in the corresponding spectrum of the wild-type enzyme, where it is associated with heme a_3, shifting to 550 nm upon binding of CO (40). In the case of R54M, the signal is also observed for the high-spin heme (Fig. 2*F*), but there is clearly also an even larger component associated with the low-spin heme (Fig. 2*E*). The latter, however, is not a spectral feature of heme *a* but arises from a different heme species that partially occupies the low-spin site (see below).

Heme Composition—Fig. 3 shows the reduced-minus-oxidized spectrum of R54M in alkaline pyridine solution. Beside the large peak at 587 nm due to heme A, there are also bands, although somewhat smaller, at 552 and 521 nm. The latter two bands can clearly not be associated with A-type heme and must therefore arise from a different heme species. The signal at 566 nm in the spectrum of the protein in aqueous solution suggests the presence of a B-type heme. Heme B, however, would be expected to give a signal at 556 nm in the pyridine hemochrome

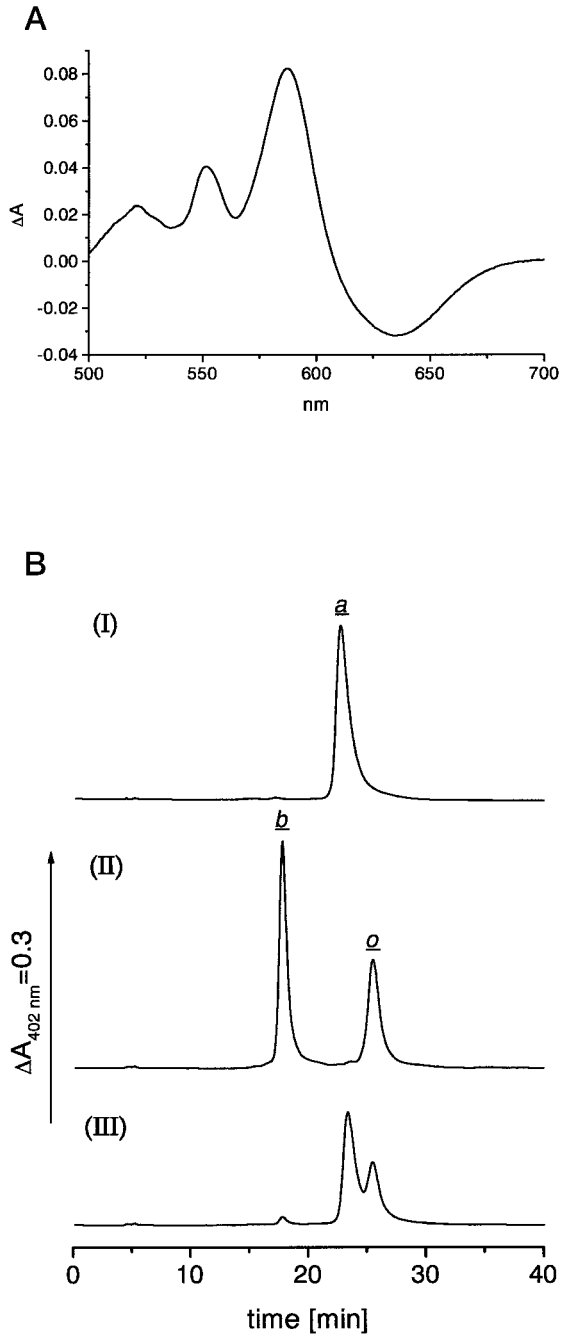

FIG. 3. **Pyridine hemochrome spectrum of R54M and HPLC elution profile of extracted hemes.** *A,* reduced-minus-oxidized difference spectrum of the R54M mutant enzyme in 0.2 M NaOH/pyridine (3:1). The protein concentration was 3.8 μM. *B,* reversed-phase HPLC elution profiles of hemes extracted from purified (*I*) wild-type *P. denitrificans* cytochrome aa_3; (*II*) *E. coli* cytochrome bo_3; (*III*) R54M mutant enzyme. Absorption was monitored at 402 nm.

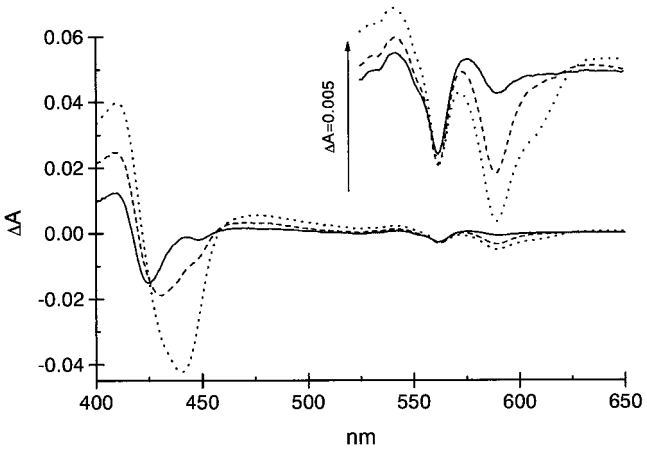

FIG. 4. **Electrochemically induced oxidized-minus-reduced difference spectra of the R54M mutant enzyme for the potential steps from −0.3 to 0 V (*solid line*, heme *o* oxidized), from −0.3 to 0.2 V (*dashed line*, hemes *o* and *a* oxidized), and from −0.3 to 0.6 V (*dotted line*, hemes *o*, *a* and a_3 oxidized.** Experimental conditions were as described by Hellwig *et al.* (35). Potentials are given *versus* SHE′.

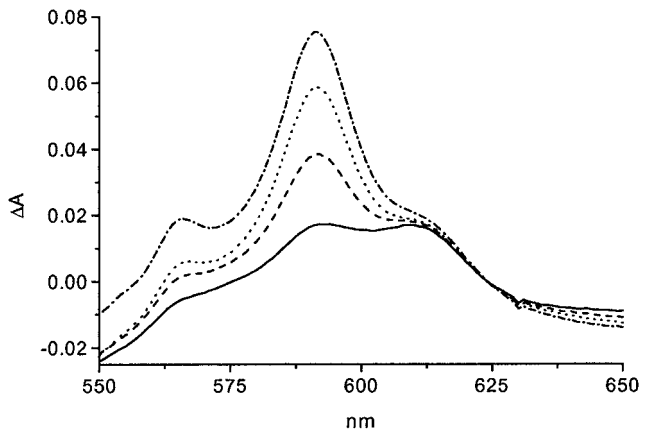

FIG. 5. **Optical difference spectra in the α-band region after addition of sodium dithionite to 7 μM of oxidized R54M.** Spectra were collected immediately (*solid line*), 5 (*dashed line*), 15 (*dotted line*), and 25 min (*dashed-dotted line*) after addition of the reductant, and the difference spectra shown were obtained by subtracting the spectrum of the oxidized enzyme.

difference spectrum which is not observed for R54M. C-type heme can also be ruled out because then a signal at 550–552 nm would have to be expected in both aqueous and pyridine solution spectra. Thus the 552/566 nm species in the pyridine/aqueous solution spectra is probably due to a heme of type O, as the absorption wavelengths are very similar to those reported for cytochrome bo_3 from *E. coli* (41). By using difference extinction coefficients of 24 mM^{-1} cm^{-1} for the peak-minus-trough (552–535 nm) absorbance difference for the O-type pyridine hemochrome (42) and 25 mM^{-1} cm^{-1} for the corresponding heme A signal (587–620 nm, Ref. 31), a ratio of 1:4 (O:A) is calculated.

The identity of the additional heme species as heme O was unequivocally confirmed by heme extraction and subsequent HPLC analysis using heme extracts from wild-type *P. denitrificans* cytochrome aa_3 and *E. coli* cytochrome bo_3 as controls (see Fig. 3*B*).

Assignment of this heme species to either the low- or the high-spin site of the mutant enzyme is difficult as the absorbance band of heme O in aqueous solution is, as mentioned above, overlaid by the 565-nm signal of the reduced heme a_3. Nevertheless, it can be concluded that the heme O contribution must predominantly, if not exclusively, be associated with the low-spin site, due to the following reasons. First, the reduced-minus-(reduced + CO) and (oxidized + CO)-minus-oxidized spectra of wild type and R54M are almost indistinguishable (*cf.* Fig. 2, *C* and *F*), indicating that there are no significant differences in heme composition and environment at the high-spin heme-binding site. Second, from the electrochemically induced difference spectra (*cf.* Fig. 4), it can be deduced that the O-type heme titrates as a single species at a potential close to that of heme *a* (see below). Finally, there is a signal at 566 nm in the (reduced + CO)-minus-(oxidized + CO) spectrum (Fig. 2*E*) that obviously cannot be due to the binuclear center heme. The low intensity of the signal in the (reduced + CO)-minus-(oxidized + CO) spectrum, as compared with the electrochemically induced and the pyridine hemochrome spectra, is most probably a result of the very low redox potential of this heme species (see below) and the correspondingly incomplete reduction.

Influence of the Mutation on Redox Potential—Loss of the positive charge very close to heme *a* was predicted to lead to a drastic decrease in the redox potential of the heme (24). And indeed, a midpoint potential for heme *a* of only 50 mV was determined in the R54M mutant, compared with 430 mV for the wild-type enzyme (35). The heme *o* potential was found to be even smaller (−20 mV). For heme a_3, the redox potential was 180 mV in the wild-type and 290 mV in the mutant enzyme. The difference in the low-spin heme potentials and especially the rise in the potential of heme a_3, with which Arg-54 does not directly interact, seem exceptionally large. However, since in the wild-type enzyme the redox potential of heme a_3 is lower than that of heme *a*, the high-spin heme is (in an oxidative titration) oxidized first, whereas the reverse is the case for the R54M mutant. Thus, in wild type the potential of the low-spin heme is determined when heme a_3 is already oxidized, whereas it is still reduced in the mutant. However, there is a negative redox cooperativity between heme *a* and the binuclear center (43), *i.e.* oxidation of the former thermodynamically disfavors oxidation of the latter and vice versa the potential of the component that is oxidized later has to be corrected for the interaction energy between the two redox centers. Therefore, when assuming this interaction energy to be ≈120 mV as described by Wilson *et al.* (44), the corrected redox potentials are 50/310 and 170/180 mV for hemes *a* and a_3 of R54M/wild type, respectively. Thus the redox potential of heme a_3 is only slightly affected by the mutation, whereas the heme *a* potential drops by ≈260 mV upon introduction of the mutation. The latter agrees well with the results of electrostatic calculations (24), as the calculated Arg-54/heme *a* interaction energy of 4.1 ΔpK units is equivalent to 246 mV.

Electron Transfer Kinetics—Fig. 5 displays the spectral changes in the α-band region of the R54M absorbance spectrum after addition of dithionite to the oxidized enzyme. Clearly, the two bands at 566 and 592 nm evolve only very slowly after addition of the reductant, whereas the 612-nm signal occurs almost instantaneously. It is thus evident (and in good agreement with the obtained redox potentials) that heme a_3 is rapidly reduced, whereas heme *a* reduction is very slow in the R54M mutant. The same effect was observed when ascorbate/cytochrome *c* or $[Ru(II)(NH_3)_6]$/cytochrome *c* were used as reductants. In these cases, reduction of the low-spin heme was not only slow but also incomplete.

Fig. 6 depicts the kinetic traces obtained when following the 1:1 reaction of cytochrome *c* with cytochrome *c* oxidase at high ionic strength in a stopped-flow spectrophotometer. In the reaction of the wild-type enzyme, the kinetics of cytochrome *c* oxidation (followed at 550 nm) is biphasic. Reduction of heme *a* can be followed at 605 nm, and its rate constant was found to be identical to that of the fast phase of cytochrome *c* oxidation (25

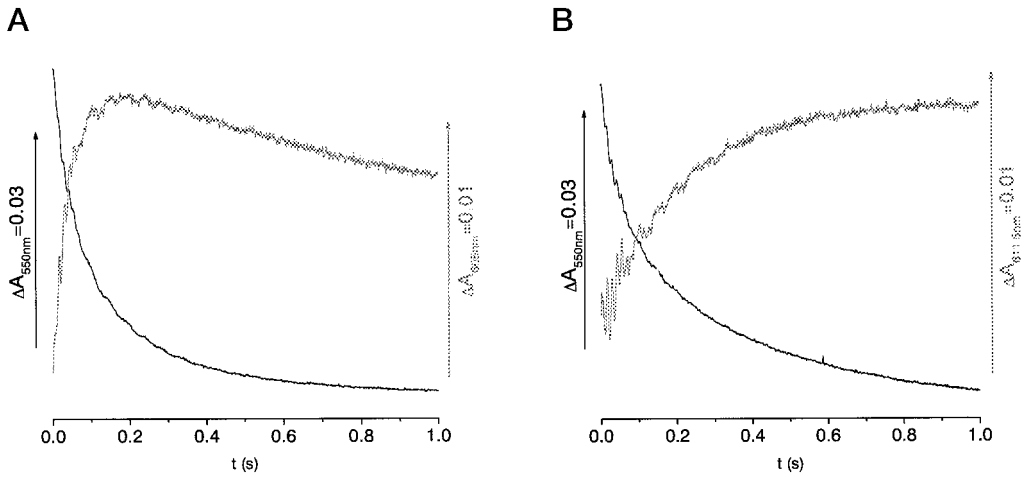

FIG. 6. **Cytochrome *c* oxidation and heme reduction followed at 550 nm (*black*) and 605(*A*) or 611.5 (*B*) nm (*gray, i.e.* the wavelengths where the respective absorbance changes are maximal, see Fig. 7) in a stopped-flow spectrophotometer.** The reaction was started by mixing equal volumes of 5 μM reduced horse heart cytochrome *c* and 5 μM cytochrome *c* oxidase in 50 mM Hepes-KOH, pH 7.3, 0.05% *n*-dodecyl-β-D-maltopyranoside, 120 mM KCl at 25 °C. *A,* wild-type; *B,* R54M mutant enzyme.

s^{-1}), indicating that the Cu_A-heme *a* electron transfer is very fast and its kinetics cannot be resolved under the experimental conditions used. In the case of the R54M mutant enzyme, cytochrome *c* oxidation was triphasic, with the rates of the two fast phases being equal to those observed for the wild-type enzyme. The latter indicates that the rate of cytochrome *c*-Cu_A electron transfer is not significantly influenced by the mutation. However, when following the reaction in the wavelength region around 600 nm, it becomes evident that the rate of heme reduction is slower in R54M (4 s^{-1}). Moreover, as shown in Fig. 7, the maximal change in absorbance did not occur at 592 nm (*i.e.* the position of the α-band of heme *a*) but at 612 nm (*i.e.* the position of the heme a_3 α-band). This, and the absence of any transient signal at 592 nm, suggests that in the R54M mutant enzyme electron transfer from Cu_A to the binuclear center does not occur via heme *a* but that instead direct electron transfer to the high-spin heme is the dominating process.

Black Lipid Membrane Experiments—Fig. 8*B* shows the electrogenic processes associated with flash-induced reduction of the R54M mutant cytochrome *c* oxidase. Injection of a single electron into R54M via excitation of Rubpy gives rise to the generation of an electric potential across the BLM, the sign of which is consistent with the translocation of negative charges from the outside to the inside of the vesicles or, correspondingly, of positive charges in the opposite direction. In comparison with the wild-type enzyme where two phases with $\tau_1 = 20$ μs and $\tau_2 = 150$ μs are observed (Fig. 8*A*), $\Delta\psi$ generation is very slow in the R54M mutant, occurring at a rate of 3–4 s^{-1}. Furthermore, the signal obtained with the R54M mutant enzyme, in contrast to that observed for the wild type, was completely inhibited in the presence of KCN. The latter binds to heme a_3 and thereby prevents electron transfer to the binuclear center but not to the low-spin heme. Thus, the complete absence of an electrical signal in the presence of potassium cyanide shows that the electric response of the R54M enzyme was solely due to electron transfer (and possibly associated proton transfer) to the binuclear center without any significant contribution from Cu_A-heme *a* electron transfer.

DISCUSSION

Mutation of arginine 54 to methionine yielded an enzyme of very low cytochrome *c* oxidase activity, with altered spectral properties, partial incorporation of heme O, drastically modified redox properties of the low-spin heme, and correspondingly, a low-spin heme that is difficult to reduce.

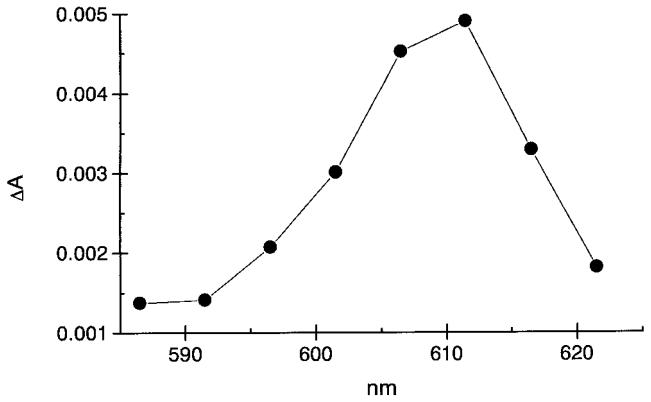

FIG. 7. **Kinetic spectrum depicting the changes in absorbance at the indicated wavelengths observed upon 1:1 mixing of ferrocytochrome *c* and R54M mutant cytochrome *c* oxidase.** Experimental conditions were as described for Fig. 6; spectral contributions from cytochrome *c* were subtracted.

The position of the α-band of the reduced low-spin heme *a* shifts from 607 nm in the wild-type enzyme to 592 nm upon introduction of the mutation. A similar but not as pronounced blue-shift was reported by Callahan and Babcock (45) for the bovine heart cytochrome *c* oxidase at very high pH. They attributed this blue-shift to the deprotonation of a residue close to the heme *a* formyl group and the resulting loss of a strong hydrogen bond between the formyl moiety and this residue. They also proposed that the red-shift of the α-band from 587 nm for the isolated heme A to 605 nm when the heme is incorporated into the protein is mainly the result of such a strong hydrogen bond. Thus, the position of the band at 592 nm in the R54M mutant is in excellent agreement with the results of Callahan and Babcock (45), and it can be further specified that the residue in question is indeed arginine 54 and not, as suggested in Ref. 45, a tyrosine.

Partial occupation of the low-spin heme-binding site with heme O can also be explained with the loss of the arginine as a hydrogen bond donor to the formyl group of the heme. The difference between hemes A and O is exactly the substituent at position 8 that is a formyl group in heme A (46) but a methyl group in heme O. This makes heme O more hydrophobic and causes its hemochrome absorbance to be shifted more to the blue range than that of heme A (with a formyl group at position 8) or heme B (that lacks the hydroxyethylfarnesyl chain; Ref.

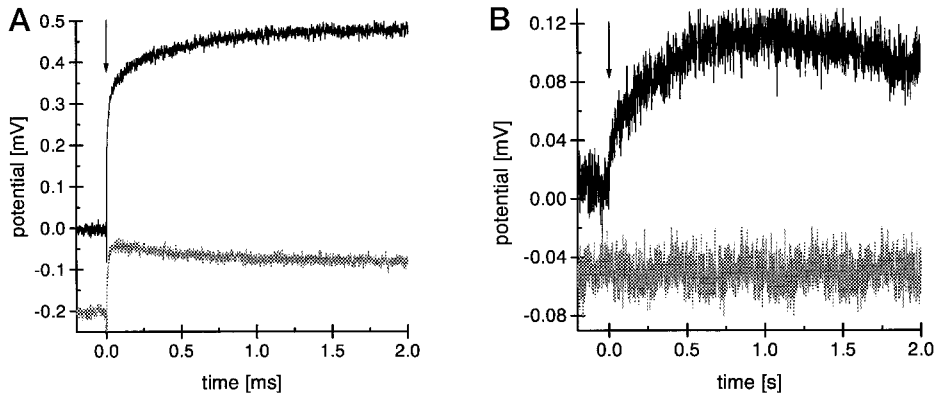

FIG. 8. **Flash-induced membrane potential generation by wild-type (*A*) and R54M mutant (*B*) cytochrome *c* oxidase.** Proteoliposomes containing the mutant enzyme (120 nM in 50 mM Hepes-KOH, pH 7.4) were attached to a BLM and subjected to a single laser pulse (451 nm, 1.60 mJ/cm^2, indicated by the *black arrow*) in the presence of 80 μM Rubpy and 300 μM EDTA. The *gray curves* represent the corresponding signals obtained in the presence of 2 mM KCN (offset by -0.2 and -0.05 mV, respectively, for clarity).

47). One could conjecture that Arg-54 is at least partly responsible for the preferred incorporation of heme A into the low-spin site and the stabilization of the bound heme, as it provides a more polar environment and forms a strong hydrogen bond to the formyl substituent. In the mutant, however, this stabilization is lost, and consequently, partial incorporation of heme O can occur. This is also plausible in the light of Arg-54 being conserved among terminal heme-copper oxidases with an A-type low-spin heme.

Replacement of heme A by heme O was shown to occur in the high-spin heme sites of the ba_3-type quinol oxidase from *Acetobacter acetii* (48) and the caa_3-type cytochrome *c* oxidase from *Bacillus* PS3 (49) when the bacteria were grown under slightly air-limited conditions. The reverse (replacement of heme O by heme A) was recently observed (34) when the *cyo* operon coding for the bo_3-type quinol oxidase in *E. coli* (which cannot produce A-type hemes) was expressed in *P. denitrificans*. In all three cases, however, the change in heme type was restricted to the high-spin heme site. In contrast, depending on the bacterial strain used and the growth conditions applied, variable amounts of hemes B and O were found in the low-spin heme site of cytochrome bo_3 from *E. coli* (42).

However, as wild-type and R54M mutant enzyme were grown under identical conditions, it can be concluded that the partial heme A $\rightarrow$ O exchange is not a result of a difference in bacterial strains or growth conditions but rather due to the mutation itself.

Of special interest is the electron transfer behavior of R54M. From Fig. 5, it can be seen that, due to its high midpoint potential, the low-spin heme is difficult to reduce. Furthermore, the results of the stopped-flow experiments (*cf.* Figs. 6 and 7) and the charge translocation measurements on the BLM (*cf.* Fig. 8) suggest that electrons from Cu_A are transferred directly to heme a_3, without transient reduction of the low-spin heme.

An alternative interpretation would be that electron transfer from Cu_A occurs via heme *a*, but the reduced heme *a* species is not detectable due to large driving force of the heme *a*-heme a_3 electron transfer and the corresponding fast rate of this process. In the light of the reduction behavior and especially the inhibition of $\Delta\psi$ generation in the presence of KCN (Fig. 8), this scenario seems rather unlikely, although it cannot be ruled out completely.

The reason for the occurrence of direct Cu_A-heme a_3 electron transfer is the very low redox potential of heme *a*, due to which the driving force of the Cu_A-heme *a* electron transfer is dramatically reduced, even inverted. The rate of electron transfer between two centers A and B depends upon driving force, reorganization energy, and distance between the redox centers according to Equation 1.

$$k_{et} = \frac{2\pi}{\hbar} \cdot V_{AB}^2 \cdot \frac{1}{\sqrt{4\pi\lambda k_B T}} \cdot e^{\frac{-(\lambda+\Delta G)^2}{4\lambda k_B T}} \qquad \text{(Eq. 1)}$$

with V_{AB} being the electronic coupling matrix element, λ the reorganization energy, and ΔG the driving force of the electron transfer reaction. The value of V_{AB} depends on the extent of the overlap of the donor and acceptor electronic wave functions and therefore on the distance separating the two redox centers.

A back-of-the-envelope estimation of the effect of the R54M mutation on k_{et} can be performed taking for the reorganization energy λ a value of 0.3 eV (29 kJ/mol) as suggested by Brzezinski (13), 250 mV as the value for the Cu_A midpoint potential (50, 51), and 310/50 mV as the redox potential of heme *a* in wild type/R54M, yielding that k_{et} is expected to be slowed down by a factor of at least 500 in the mutant compared with the wild-type enzyme. Note, however, that this value can only be a very rough estimate as it is based on quite a number of simplifying assumptions. Nevertheless, it suggests that Cu_A-heme *a* electron transfer is slowed down by at least 2–3 orders of magnitude in the R54M mutant compared with the wild-type cytochrome *c* oxidase and makes the observation of direct Cu_A-heme a_3 electron transfer in the R54M mutant enzyme plausible.

Papa *et al.* (19) have suggested a regulatory function of this "direct" electron transfer reaction for the stoichiometry of proton pumping. They proposed that, even in the wild-type enzyme where, under normal conditions, Cu_A-heme *a* electron transfer is at least 100-fold faster than Cu_A-heme a_3 electron transfer, the latter may occur to a significant extent at high $\Delta\mu_{H^+}$. This could cause a "slip" in the proton pump as proton uptake associated with heme *a* reduction would be partially abolished, yielding H^+/e^- proton-pumping stoichiometries of less than unity. It would therefore be of interest to test whether the R54M mutant enzyme reconstituted into proteoliposomes is able to pump protons and what the pump stoichiometry would be. However, due to the low turnover number of R54M, proton pumping is difficult to measure, as passive proton flow across the vesicular membrane will obstruct the acidification signal associated with proton pumping. It may, however, be possible to conduct proton pumping measurements using enzyme reconstituted in vesicles with low proton permeability. Such experiments are under way.

Acknowledgments—We are grateful to Hannelore Müller and Hans-Werner Müller for technical assistance and to Dr. Ron Clarke and Christian Lüpfert for help with the stopped-flow spectrophotometer. We

thank Hans Rogl and Thomas Ostermann for help with the HPLC heme analysis. Julia Behr and Axel Harrenga are acknowledged for careful reading of the manuscript.

REFERENCES

1. Michel, H., Behr, J., Harrenga, A., and Kannt, A. (1998) *Annu. Rev. Biophys. Biomol. Struct.* **27,** 329–356
2. Hill, B. C. (1994) *J. Biol. Chem.* **269,** 2419–2425
3. Geren, L. M., Beasley, J. R., Fine, B. R., Saunders, A. J., Hibdon, S., Pielak, G. J., Durham, B., and Millett, F. (1995) *J. Biol. Chem.* **270,** 2466–2472
4. Hazzard, J. T., Rong, S.-Y., and Tollin, G. (1991) *Biochemistry* **30,** 213–222
5. Witt, H., Malatesta, F., Nicoletti, F., Brunori, M., and Ludwig, B. (1998) *Eur. J. Biochem.* **251,** 367–373
6. Winkler, J. R., Malmström, B. G., and Gray, H. B. (1995) *Biophys. Chem.* **54,** 199–209
7. Ädelroth, P., Ek, M., Brzezinski, P. (1998) *Biochim. Biophys. Acta* **1367,** 107–117
8. Iwata, S., Ostermeier, C., Ludwig, B., and Michel, H. (1995) *Nature* **376,** 660–669
9. Moody, A. J., Brandt, U., and Rich, P. R. (1991) *FEBS Lett.* **293,** 101–105
10. Larsson, S., Källebring, B., Wittung, P., and Malmström, B. G. (1995) *Proc. Natl. Acad. Sci. U. S. A.* **92,** 7167–7171
11. Ramirez, B. E., Malmström, B. G., Winkler, J. R., and Gray, H. B. (1995) *Proc. Natl. Acad. Sci. U. S. A.* **92,** 11949–11951
12. Regan, J. J., Ramirez, B. E., Winkler, J. R., Gray, H. B., and Malmström, B. G. (1998) *J. Bioenerg. Biomembr.* **30,** 35–40
13. Brzezinski, P. (1996) *Biochemistry* **35,** 5611–5615
14. Verkhovsky, M. I., Morgan, J. E., and Wikström, M. (1995) *Biochemistry* **34,** 7483–7491
15. Antalis, T. M., and Palmer, G. (1982) *J. Biol. Chem.* **257,** 6194–6206
16. Oliveberg, M., and Malmström, B. G. (1991) *Biochemistry* **30,** 7053–7057
17. Ädelroth, P., Brzezinski, P., and Malmström, B. G. (1995) *Biochemistry* **34,** 2844–2849
18. Babcock, G. T., and Callahan, P. M. (1983) *Biochemistry* **22,** 2314–2319
19. Papa, S., Capitanio, N., and Villani, G. (1998) *FEBS Lett.* **439,** 1–8
20. Michel, H. (1998) *Proc. Natl. Acad. Sci. U. S. A.* **95,** 12819–12824
21. Yoshikawa, S., Shinzawa-Itoh, K., Nakashima, R., Yaono, R., Yamashita, E., Inoue, N., Yao, M., Fei, M. J., Libeu, C. P., Mizushima, T., Yamaguchi, H., Tomizaki, T, and Tsukihara, T. (1998) *Science* **280,** 1723–1729
22. Ostermeier, C., Harrenga, A., Ermler, U., and Michel, H. (1997) *Proc. Natl. Acad. Sci. U. S. A.* **94,** 10547–10553
23. Tsukihara, T., Aoyama, H., Yamashita, E., Tomizaki, T., Yamaguchi, H., Shinzawa-Itoh, K., Nakashima, R., Yaono, R., and Yoshikawa, S. (1996) *Science* **272,** 1136–1144
24. Kannt, A., Lancaster, C. R. D., and Michel, H. (1998) *Biophys. J.* **74,** 708–721
25. Pfitzner, U., Odenwald, A., Ostermann, T., Weingard, L., Ludwig, B., and Richter, O.-M. H. (1998) *J. Bioenerg. Biomembr.* **30,** 89–97
26. Ludwig, B. (1986) *Methods Enzymol.* **126,** 153–159
27. Gerhus, E., Steinrücke, P., and Ludwig, B. (1990) *J. Bacteriol.* **172,** 2392–2400
28. Kleymann, G., Ostermeier, C., Ludwig, B., Skerra, A., and Michel, H. (1995) *Bio/Technology* **13,** 155–160
29. Voss, S., and Skerra, A. (1997) *Prot. Engineering* **10,** 975–982
30. Bartsch, R. G. (1971) *Methods Enzymol.* **23,** 344–363
31. Berry, E. A., and Trumpower, B. L. (1987) *Anal. Biochem.* **161,** 1–15
32. Puustinen, A., Finel, M., Haltia, T., Gennis, R. B., and Wikström, M. (1991) *Biochemistry* **30,** 3936–3942
33. Weinstein, J. D., and Beale, S. I. (1983) *J. Biol. Chem.* **258,** 6799–6807
34. Schröter, T., Winterstein, C., Ludwig, B., and Richter, O.-M. H. (1998) *FEBS Lett.* **432,** 109–112
35. Hellwig, P., Grzybek, S., Behr, J., Ludwig, B., Michel, H., and Mäntele, W. (1999) *Biochemistry* **38,** 1685–1694
36. Bamberg, E., Apell, H. J., Dencher, N. A., Sperling, W., Stieve, H., and Läuger, P. (1979)*Biophys. Struct. Mechanism* **5,** 277–292
37. Hartung, K., Froehlich, J., and Fendler, K. (1997) *Biophys. J.* **72,** 2503–2514
38. Gropp, T., Cornelius, F., and Fendler, K. (1998) *Biochim. Biophys. Acta* **1368,** 184–200
39. Nilsson, T. (1992) *Proc. Natl. Acad. Sci. U. S. A.* **89,** 6497–6501
40. Vanneste, W. H. (1966) *Biochemistry* **5,** 838–848
41. Puustinen, A., and Wikström, M. (1991) *Proc. Natl. Acad. Sci. U. S. A.* **88,** 6122–6126
42. Puustinen, A., Morgan, J. E., Verkhovsky, M. I., Thomas, J. W., Gennis, R. B., and Wikström, M. (1992) *Biochemistry* **31,** 10363–10369
43. Wikström, M., Krab, K., and Saraste, M. (1981) *Cytochrome Oxidase-a Synthesis,* pp. 88–115, Academic Press, New York
44. Wilson, D. F., Lindsay, J. G., and Brocklehurst, E. S. (1972) *Biochim. Biophys. Acta* **256,** 277–286
45. Callahan, P. M., and Babcock, G. T. (1983) *Biochemistry* **22,** 452–461
46. Caughey, W. S., Smythe, G. A., O'Keeffe, D. H., Maskasky, J. E., and Smith, M. L. (1975) *J. Biol. Chem.* **250,** 7602–7622
47. Mogi, T., Saiki, K., and Anraku, Y. (1994) *Mol. Microbiol.* **14,** 391–398
48. Matsushita, K., Ebisuya, H., and Adachi, O. (1992) *J. Biol. Chem.* **267,** 24748–24753
49. Sone, N., and Fujiwara, Y. (1991) *FEBS Lett.* **288,** 154–158
50. Tsudzuki T., and Wilson, D. F. (1971) *Arch. Biochem. Biophys.* **145,** 149–154
51. Hartzell, C. R., and Beinert, H. (1976) *Biochim. Biophys. Acta* **423,** 323–338
52. Kannt, A., Lancaster, C. R. D., and Michel, H. (1998) *J. Bioenerg. Biomembr.* **30,** 81–87
53. Nicholls, A., Sharp, K. A., and Honig, B. (1991) *Proteins* **11,** 281–296